Applied Catalysis B: Environmental 192 (2016) 108–115

Contents lists available at ScienceDirect

Applied Catalysis B: Environmental

journal homepage: www.elsevier.com/locate/apcatb

Modulation of peripheral substituents of cobalt thioporphyrazines and their photocatalytic activity

Quan Zhou, Shuai Xu, Changjun Yang*, Bingguang Zhang, Zhe Li, Kejian Deng*

Key Laboratory of Catalysis and Material Sciences of the State Ethnic Affairs Commission & Ministry of Education, College of Chemistry and Material Sciences, South-Central University for Nationalities, Wuhan 430074, China

ARTICLE INFO

Article history:
Received 10 January 2016
Received in revised form 21 March 2016
Accepted 24 March 2016
Available online 26 March 2016

Keywords:
Substituted thioporphyrazines
Biomimetic catalyst
Activating dioxygen
Synthesis and characterization
Photocatalytic behaviour

ABSTRACT

A series of thioporphyrazines have been synthesized via cocondensation from 2,3-dicyano-1,4-dithiin (A) and 2,3-bis(butylthio) maleonitrile (B) and thoroughly characterized with UV–vis, ^{1}H NMR and MALDI-TOF MS. Through modulation of peripheral substituents of thioporphyrazines, both symmetrical and asymmetrical molecular structures in thioporphyrazines including B_4, *cis*-A_2B_2, *trans*-A_2B_2 and AB_3 were obtained, and were further used to react with cobalt acetate to form metal complexes, cobalt thioporphyrazines. Moreover, they were loaded on Al_2O_3 to form biomimetic catalysts for photocatalytic activation of dioxygen, whose efficiencies were assessed by photodegradation of Rhodamine B (RhB) in an aerated suspension under simulating sunlight irradiation. Importantly, it was found that the lower on the molecular symmetry of thioporphyrazine delivers the better on the photocatalytic activity. Electrochemical and theoretical studies demonstrated that lowering the molecular symmetry of the cobalt thioporphyrazines moderately decreased the HOMO-LUMO energy gap and increased the contribution of S atom in substitiuents to HOMO so as to enhance the photocatalytic activity. A possible mechanism to predict this reaction pattern was proposed through both detailed analysis of degradation products by HPLC and detection of the main reactive oxygen species (ROS) by ESR, indicating both energy transfer (major) and electron transfer (minor) to dioxygen to exist in the heterogeneous light photocatalytic system.

1. Introduction

Metalloporphyrin and metallophthalocyanine with an extended delocalized π-electron conjugated macrocyclic system are well known for their electron-transfer and photosensitive roles in a myriad of redox systems in nature [1]. Tetraazaporphyrin or porphyrzine (Pz) which is a member of the porphyrin family has similar topology of tetrapyrrolic ring to porphyrin and phthalocyznine, but has obviously different chemical behavior. Among them, thioporphyrazine exhibits some unique electronic and optical properties that differ from their porphyrin counterparts owing to the β-position sulfur-containing groups in periphery and *meso* N atoms to replace methine groups leading to contraction of the central cavity. It suggests the importance of structure subtlety in conjugated macrocyclic system in tuning the properties. Therefore, the synthesis and application of porphyrazines and thioporphyrazines with unique performace is still a challenge [2]. Our research group has recently found that thioporphyrazine exhibited a high thermal stability and unique photocatalytic activity for activating hydrogen peroxide and dioxygen [3–7]. Herein, we want to further investigate the molecular structure of thioporphyrazine through modulation of peripheral substituents so as to define the final photocatalytic activity.

According to the principle of crystallography, low-symmetrical structure could exhibit special physical, chemical and photoredox properties [8]. Among porphyrazines, however, the accessibility of the low-symmetrical porphyrazine is much harder than the symmetrical one [9]. To investigate the effect of molecule structure on the photocatalytic activity of metal thioporphyrazine, the symmetrical and asymmetrical metal thioporphyrazines were synthesized by introducing different type and quantity of substituent groups onto the periphery of macrocycle. Specifically, two different maleonitriles were designed to be chosen in present work: one of which is 2,3-dicyano-1,4-dithiin to be able to promote catalytic activity via periphery; the other of which is 2,3-bis(butylthio)-maleonitrile to be able to promote solubility of the porphyrazine macrocycle. And a thorough comparison of physical and chemical properties of these

* Corresponding authors.
E-mail addresses: yangchangjun@mail.scuec.edu.cn (C. Yang), dengkj@scuec.edu.cn (K. Deng).

http://dx.doi.org/10.1016/j.apcatb.2016.03.059
0926-3373/

prepared thioporphyrazines was made. In addition, neutral Al_2O_3 particles were chosen as the support for cobalt thioporphyrazines to form biomimetic heterogeneous catalysts. In the end, their photocatalytic activities were evaluated by oxidative degradation of dye Rhodamine B (RhB) under simulating sunlight irradiation in an aerated suspension.

Organic dyes are commonly present in textile, paper and printing industry effluents. However, most of the organic dyes are not readily biodegradable which present an immediate threat to aquatic life and human beings [10–12]. Hence, great attention has been paid to oxidative degradation of persistent organic dyes from wastewater because of its high mineralization efficiency [13,14]. With special attention to metalloporphyrin and metallophthalocyanine-based potocatalysts, because these technologies could use sunlight and dioxygen for the removal of persistent dye pollutants [15–17]. In our previous research, thioporphyrazines have also been proven to be excellent photocatalysts for the oxidation degradation of organic pollutants under sunlight [5–7]. In this paper, the factor of molecular structure of cobalt thioporphyrazine loaded on Al_2O_3 was examined in detail to gain fundmental insight in the application of metalloporphyrin as a biomimetic photocatalyst, opening a new door for the removal of persistent dye pollutants by using sunlight and air, and it is also a reference for photodynamic therapy of cancers.

2. Experimental

2.1. Synthesis of low-symmetrical metal-free thioporphyrazines

Porphyrazine formation is widely used the Linstead macrocyclization, and two different maleonitriles via cocondensation could form the mixed cyclization to obtain different porphyrazines including the molecules of symmetrical and asymmetrical structure. In a typical synthetic strategy, the precursors 2,3-dicyano-1,4-dithiin (0.6460 g, 4 mmol) and 2,3-bis(butylthio)maleonitrile (0.5000 g, 2 mmol) were mixed in magnesium butoxide (100 mL). Then the mixture was stirred at reflux under nitrogen for 48 h, the crude solid formed was filtered and washed with methanol until the filtrate being colorless, giving mixed products of 1a, 2a, 3a and 4a.

Subsequently, the mixed products were dissolved in 50 mL trifluoroacetic acid (TFA), and further stirred 12 h in dark so as to remove the center metal magnesium. Then the solution was poured into purified water to precipitate the target metal-free thioporphyrazine. The dark purple products were obtained by washing with ammonia solution (10%), purified water and methanol in sequence. Four thioporphyrazines, sunch as 1b, 2b, 3b and 4b, could be effectively obtained by separating the above products on chromatography column with silica gel using dichloromethane (CH_2Cl_2)/petroleum ether (PE) (3:1, v/v) as eluent. The target products 1b, 2b, 3b and 4b were characterized with UV–vis spectrum, ^{1}H NMR spectrum and MALDI-TOF MS, the characteristic structure datas for the products were shown as following:

Product 1b: tetra(2,3-bis(butylthio)maleonitrile) porphyrazine, denoted as B_4

0.2 g (yield 10%); UV–vis λ_{max} (in CH_2Cl_2): Q-band: 712 nm and 641 nm; Soret-band: 508 nm, B-band: 349 nm; ^{1}H NMR (400 MHz, $CDCl_3$): δ = 4.106 (t, 2H, $-SCH_2$-), 1.873 (m, 2H, $-CH_2$-), 1.613 (m, 2H, $-CH_2$-), 0.935 (t, 3H, $-CH_3$), −1.099 (t, 2H, −NH-); MALDI-TOF MS: m/z = 1019.3 $[M+H]^+$. See also Figs. S1 and S2 in supplementary materials.

Produt 2b: tri(2,3-bis(butylthio)maleonitrile)-(1,4-dithiin) porphyrazine, denoted as B_3A

0.1 g (yield 6%); UV–vis λ_{max} (in CH_2Cl_2): Q-band: 712 nm and 630 nm, Soret-band: 519 nm, B-band: 360 nm; ^{1}H NMR (400 MHz, $CDCl_3$): δ = 4.141 (t, 2H, $-SCH_2$-), 1.913 (m, 2H, $-CH_2$-), 1.665 (m, 2H, $-CH_2$-), 0.981 (t, 3H, $-CH_3$-), 3.765 (t, 2H, $-SCH_2$-), −2.37 (t, 2H, −NH-); MALDI-TOF MS: m/z = 934.3 $[M+H]^+$. See also Figs. S3 and S4 in supplementary materials.

Product 3b: *trans*-di(2,3-bis(butylthio)maleonitrile)-di(1,4-dithiin) porphyrazine, denoted as *trans*-B_2A_2

0.04 g (yield 2.2%); UV–vis λ_{max} (in CH_2Cl_2): Q-band: 715 nm and 614 nm, Soret-band: 522 nm, B-band: 361 nm; ^{1}H NMR (400 MHz, $CDCl_3$): δ = 4.266 (t, 2H, $-SCH_2$-), 1.922 (m, 2H, $-CH_2$-), 1.685 (m, 2H, $-CH_2$-), 0.98 (t, 3H, $-CH_3$-), 3.811 (t, 2H, $-SCH_2$-), −2.23 (t, 2H, −NH-); MALDI-TOF MS: m/z = 847.5 $[M+H]^+$. See also Figs. S5 and S6 in supplementary materials.

Product 4b: *cis*-di(2,3-bis(butylthio)maleonitrile)-di(1,4-dithiin) porphyrazine, denoted as *cis*-B_2A_2

0.06 g (yield 4.4%); UV–vis λ_{max} (in CH_2Cl_2): Q-band: 707 nm and 629 nm, Soret-band: 519 nm, B-band: 359 nm; ^{1}H NMR (400 MHz,$CDCl_3$): δ = 4.247 (t, 2H, $-SCH_2$-), 1.929 (m, 2H, $-CH_2$-), 1.683 (m, 2H, $-CH_2$-), 0.984 (t, 3H, $-CH_3$-), 3.759 ~ 3.817 (t, 2H, $-SCH_2$-), −3.58 (t, 2H, −NH-); MALDI-TOF MS: m/z = 847.2 $[M+H]^+$. See also Figs. S7 and S8 in supplementary materials.

2.2. Synthesis of low-symmetrical cobalt thioporphyrazines

Thioporphyrazine free-base (1b, 2b, 3b or 4b) (0.1000 g) and $Co(OAc)_2.4H_2O$ (0.2400 g) were respectively added into 15 mL DMF solution, the mixture was then stirred for 10 h at 70 °C. The crude solid formed was filtered and washed with purified water and methanol until the filter liquor being colorless. The target product cobalt thioporphyrazines, such as 1c, 2c, 3c and 4c, were obtained respectively by purifying the crude solid on a silica column with CH_2Cl_2 as eluent. The target products 1c, 2c, 3c and 4c were also characterized with UV–vis spectrum and MALDI-TOF MS, the characteristic structure datas for the products were shown as following:

Complex 1c: Cobalt tetra(2,3-bis(butylthio)maleonitrile) porphyrazine, denoted as CoB_4

0.08 g (yield 75%); UV–vis λ_{max} (in CH_2Cl_2): Q-band: 645 nm, Soret-band: 440 nm, B-band: 333 nm. MALDI-TOF MS: m/z = 1076.2 $[M+H]^+$. See also Fig. S9 in supplementary materials.

Complex 2c: Cobalt tri(2,3-bis(butylthio)maleonitrile)-(1,4-dithiin) porphyrazine, denoted as CoB_3A

0.07 g (yield 70%); UV–vis λ_{max} (in CH_2Cl_2): Q-band: 643 nm, Soret-band: 436 nm, B-band: 339 nm. MALDI-TOF MS: m/z = 990.2 $[M+H]^+$. See also Fig. S10 in supplementary materials.

Complex 3c: *trans*-di(2,3-bis(butylthio)maleonitrile)-di(1,4-dithiin) porphyrazine, denoted as *trans*-CoB_2A_2

0.06 g (yield 64%); UV–vis λ_{max} (in CH_2Cl_2): Q-band: 638 nm. Soret-band: 443 nm, B-band: 338 nm; MALDI-TOF MS: m/z = 904.1 $[M+H]^+$. See also Fig. S11 in supplementary materials.

Complex 4c: *cis*-di(2,3-bis(butylthio)maleonitrile)-di(1,4-dithiin) porphyrazine, denoted as *cis*-CoB_2A_2

0.07 g (yield 70%); UV–vis λ_{max} (in CH_2Cl_2): Q-band: 644 nm. Soret-band: 433 nm, B-band: 341 nm. MALDI-TOF MS: m/z = 933.2 $[M+H]^+$. See also Fig. S12 in supplementary materials.

2.3. Cyclic voltammetric characterization of cobalt thioporphyrazines

Cyclic voltammetric datas were collected using CHI650D electrochemical workstation (Chenhua Corp., Shanghai, China) using a conventional three-electrode system. A Pt wire electrode was employed as working electrode. Ag disc electrode (2 mm) was used as reference electrode and counter electrode, respectively. 1 mmol cobalt thioporphyrazine (1c, 2c, 3c or 4c) and 341 mg tetrabutylammonium perchlorate (TBAP) were respectively dissolved in 10 mL

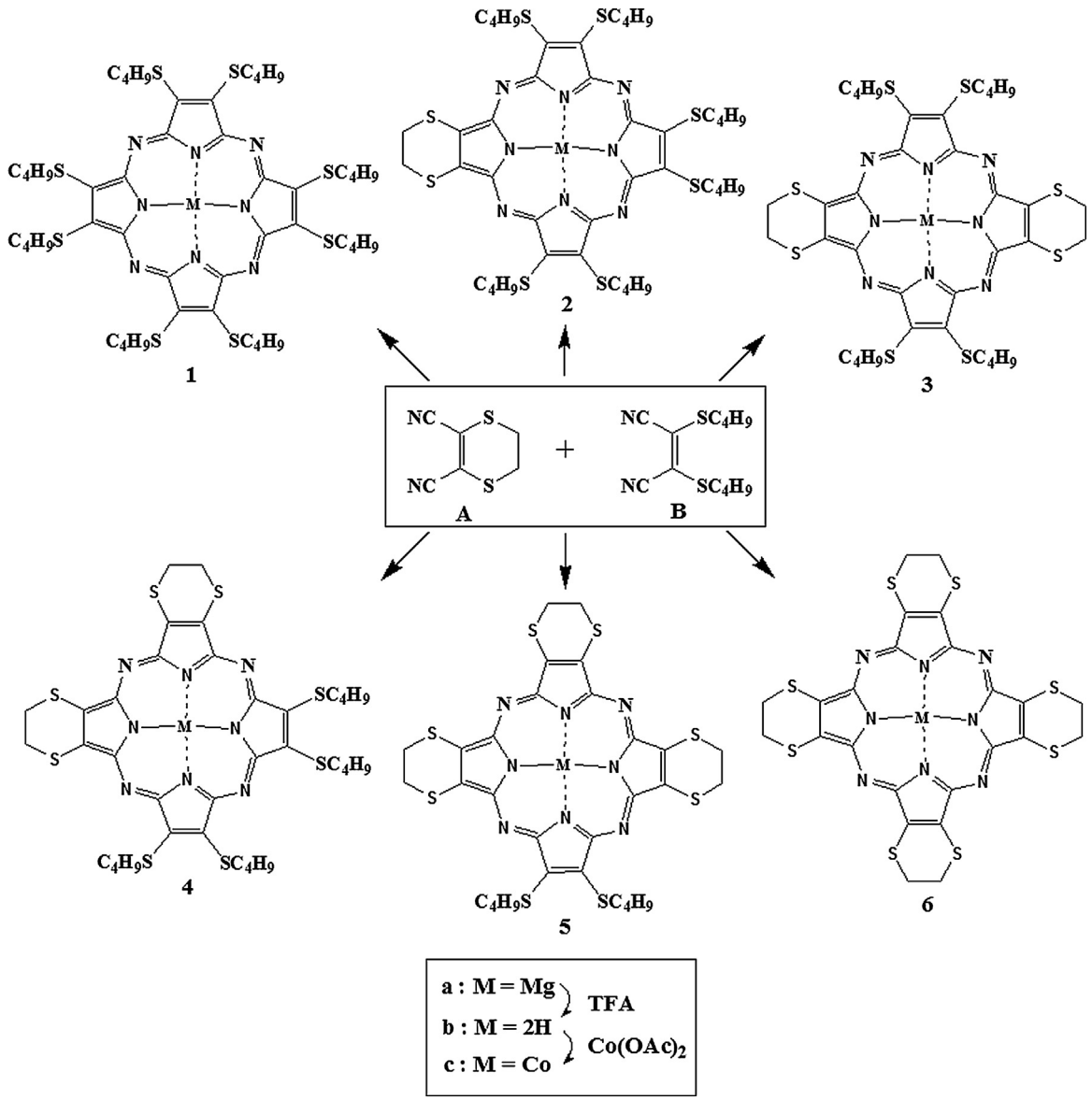

Fig. 1. Possible products of cobalt thioporphyrazines cocyclized from A and B.

CH_2Cl_2. TBAP was added as supporting electrolyte. The O_2 and H_2O in CH_2Cl_2 were removed before being used as solvent.

2.4. Preparation of Al_2O_3 loading cobalt thioporphyrazine

4.0 mg cobalt porphyrazine (1c, 2c, 3c or 4c) was firstly dissolved in 50 mL CH_2Cl_2 under ultrasonic action. Then the solution was added dropwise into a suspension containing 1.0 g activated Al_2O_3 in 50 mL CH_2Cl_2 under stirring. The stirring was continued for 24 h for adsorption equilibrium to obtain Al_2O_3 loading cobalt porphyrazine (1c, 2c, 3c or 4c). After removing the solvent CH_2Cl_2 by reduced pressure distillation, the Al_2O_3 loading cobalt thioporphyrazines were obtained finally. The content of cobalt porphyrazine (1c, 2c, 3c or 4c) loaded on the Al_2O_3 was equal to 4.0‰.

2.5. Photocatalytic degradation of RhB catalyzed by Al_2O_3 loading cobalt porphyrazine

20 mg cobalt porphyrazine loaded on Al_2O_3 was added into 50 mL RhB (1.0×10^{-5} M) at different pH values, the suspension was further stirred 12 h in dark before light irradiation to establish the adsorption equilibrium. In a typical photocatalytic reaction, the suspension containing the catalyst and RhB was irradiated under a Xe lamp (light intensity 7.0×10^4 Lumina) in an aerated suspension for 8 h. Small aliquots of the suspension were withdrawn by a syringe at given intervals of irradiation and separated from the catalyst particles by filtration, in which the concentration of RhB was then analyzed by Shimazu UV 2600 UV–vis spectrophotometer.

2.6. Analysis of degraded products of RhB using HPLC

Analysis of the degradation products of RhB was done on a VARIAN ProStar 210HPLC system. The samples were separated using a reversed-phase C18 column (200 × 4.6 mm) at 500 nm. The column temperature was maintained at 30 °C. The optimized mobile phase consisted of acetonitrile and water with the volume ratio at 90:10. The flow rate was set at 1.0 mL/min.

2.7. Theoretical calculation

Density functional theory (DFT) calculations were performed with Gaussian 09 package of programs. 36 Geometries of four cobalt

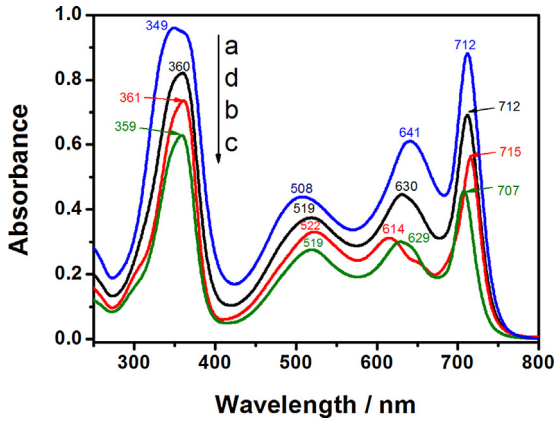

Fig. 2. UV–vis spectra of metal-free thioporphyrazines in CH_2Cl_2. a:B_4, b: *trans*-B_2A_2, c: *cis*-B_2A_2, d: B_3A..

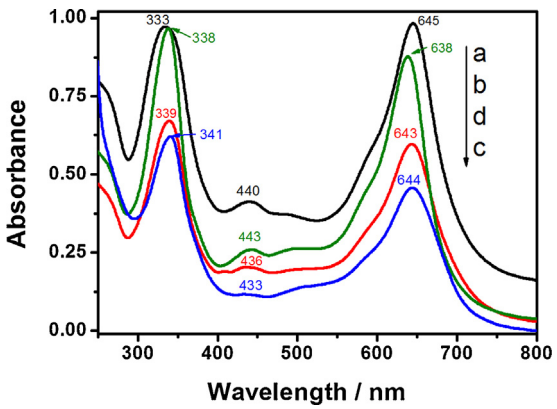

Fig. 3. UV–vis spectra of cobalt thioporphyrazines in CH_2Cl_2. a:CoB_4, b: *trans*-CoB_2A_2, c: *cis*-CoB_2A_2, d: CoB_3A.

thioporphyrazines (CoB_4, *trans*-CoB_2A_2, *cis*-CoB_2A_2 and CoB_3A) were optimized by the hybrid B3LYP functional coupled with the 6-31G* basis set, from which the frontier molecular orbitals were analyzed.

3. Results and discussion

3.1. Synthesis and characterization of thioporphyrazines and their cobalt complexes

Since its inception in 1952, the Linstead macrocyclization is still the widely used magnesium template method for porphyrazine formation [2]. In a move towards asymmetrical sulfur porphyrazines, the mixed cyclization between two different maleonitriles was developed by Hoffman group [18]. In present work, two different maleonitriles 2,3-dicyano-1,4-dithiin (A) and 2,3-bis(butylthio)-maleonitrile (B) were designed to be chosen as the precursors. The target of asymmetrical thiopophyrazines were synthesized from cocyclization of above A and B according to Linstead's magnesium template method (Fig. 1). The mole ratio of 2:1 of A to B to be biased the reaction towards the desired isomer with more A constitution. The mixture was stirred at reflux under nitrogen sufficiently to react for 48 h, forming mixed complexes with central Mg ion. After that, the mixed crude products were acidized to remove magnesium, subsequently separated by column chromatography of silica gel. The four products B_4(1), AB_3(2), *trans*-A_2B_2(3) and *cis*-A_2B_2(4) were isolated to obtain, their yields 10%, 6%, 2.2% and 4.4% respectively. There still were two products A_4 and A_3B not to be isolated according to the combination model proposed by Hoffman group should form six products from mixture of A and B [18]. Maybe the A_3B(5) and A_4(6) were not isolated to obtain for poor solubility in CH_2Cl_2. As-prepared thioporphyrazines directly reacted with cobalt acetate respectively in DMF solution to produce corresponding cobalt complexes after purifying on silica column, denoted as CoB_4, CoB_3A, *trans*-CoB_2A_2 and *cis*-CoB_2A_2, yields 75%, 70%, 64% and 70% respectively.

The UV–vis absorption spectra of metal-free thioporphyrazines and cobalt thioporphyrazines were shown in Fig. 2 and Fig. 3 respectively. These UV–vis absorption spectra show the characteristic absorption of porphyrazine, such as B-band or Soret-band produced by $n \rightarrow \pi^*$ transitions of tetrapyrrolic rings and Q-band produced by $\pi \rightarrow \pi^*$ transitions of π-electron conjugated macrocycle. Fig. 2 shows the splitting two peaks of Q-band, which is an important characteristic of free-base porphyrazine. The characteristic absorption peaks of B-band had approximate positions due to their same pyrrolic ring, but the effect of different substituents on B-band of porphyrazines caused bathochromic shift about 10 nm relative to the symmetrical B_4. Similarly, the characteristic absorption peak 508 nm produced by the $n \rightarrow \pi^*$ transition of lone-pair electron of peripheral sulfur atoms to the macrocyclic π system also red-shifted about 10 nm for asymmetrical substituents of B_3A, *trans*-B_2A_2 and *cis*-B_2A_2. It is noteworthy that the splitting of their Q-bands has two characteristics: the splitting spacing of the symmetrical B_4 is less than the one of the asymmetrical B_3A, *trans*-B_2A_2 and *cis*-B_2A_2, and the splitting spacing of the *trans*-B_2A_2 is much bigger than that of the *cis*-B_2A_2, which demonstrated that the splitting of Q-band associated with asymmetrically attached perypheral substituents [19,20].

The ^{1}H NMR spectrum of the symmetrical B_4 showed four kinds of hydrogens 4.106 (t, 2H, $-SCH_2$-), 1.873 (m, 2H, $-CH_2$-), 1.613 (m, 2H, $-CH_2$-) and 0.935 (t, 3H, $-CH_3$) in butylthio group besides inner hydrongen −1.099 (t, 2H, −NH-) of macrocycle. And the ^{1}H NMR spectrum of the asymmetrical B_3A emerged a visibly new peak at 3.765 (t, 2H, $-SCH_2$-) besides similar spectrum of the B_4, which demonstated the presence of dithiin group in pheriphery of the porphyrazine. The MALDI-TOF MS of two isomers of B_2A_2 both have m/z = 847 $[M+H]^+$, but the two kinds of hydrogens (4.366 and 3.811) of $-SCH_2$- group in butylthio substituent and in the dithiin substituent of the *trans*-B_2A_2 were not basically split while the counterparts of *cis*-B_2A_2 were split into multiplets, which demonstrated that there is bigger interaction between the substuents leading to them splitting. Their ^{1}H NMR spectra and MALDI-TOF MSs were also shown in Figs. S1-S8 in supplementary materials.

Compared with the UV–vis absorption spectra of free-base thioporphyrazines, the spectra of cobalt thioporphyrazines disappeared the splitted Q-band in CH_2Cl_2 due to the coordination with centre metal ion, as shown in Fig. 3. And unlike free-base, their complexes were not sensitive to the structure with peripheral different substituents of the macrocycle, thus respective characteristic peaks were little difference and disorder. Despite, the asymmetrical cobalt thioporphyrazines still produced hypochromatic-shift of Q-band as well as and bathochromic-shift of soret-band about several nanometers relative to those of symmetrical CoB_4. And the weak absorption peak of the cobalt thioporphyrazines produced by the $n \rightarrow \pi^*$ transition of peripheral sulfur atoms to the macrocyclic π system shifted to near 440 nm from near 508 nm of their free base. Anyway, it is observed that these cobalt thioporphyrazines showed intense absorption in the visible light region, the as-prepared cobalt thioporphyrazines could be used as photocatalysts stimulated by sunlight. The MALDI-TOF MSs of CoB_4, CoB_3A, *trans*-CoB_2A_2 and *cis*-CoB_2A_2 were respectively obtained in Figs. S9-S12 in supplementary materials.

To evaluate the photocatalytic efficiency of these cobalt thioporphyrzines, they were loaded on a carrier for their insolubility

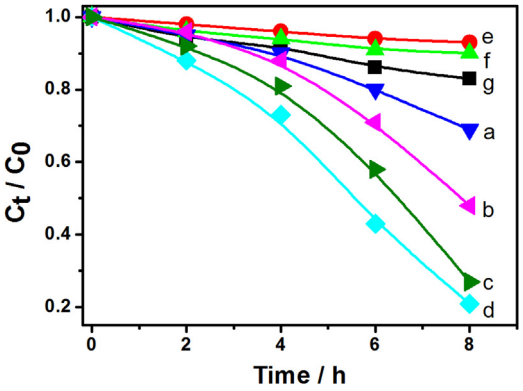

Fig. 4. Comparative experiments on the photocatalytic degradation of RhB at pH 4. a: CoB_4@Al_2O_3/air/light; b: *trans*-CoB_2A_2@Al_2O_3/air/light; c: *cis*-CoB_2A_2 @Al_2O_3/air/light; d: CoB_3A@Al_2O_3/air/light; e: CoB_3A@Al_2O_3/N_2/light; f: CoB_3A@Al_2O_3/air/dark; g: air/light.

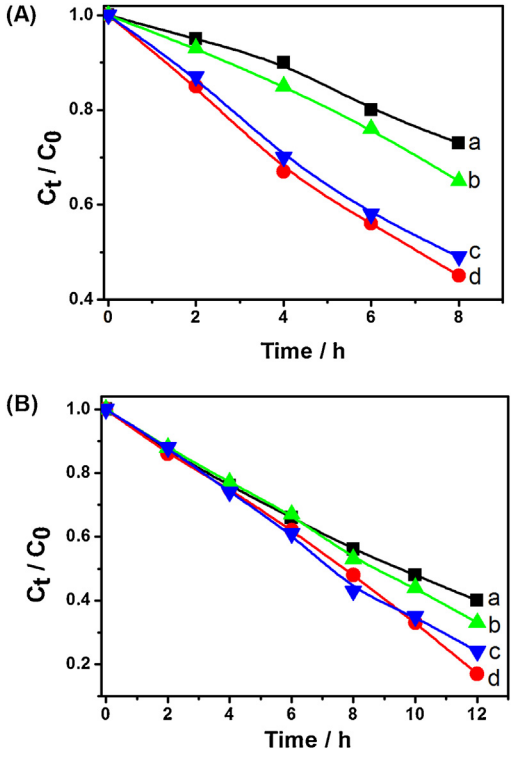

Fig. 5. Comparative experiments on the photocatalytic degradation of RhB at pH 6.8 (A) and at pH 9.12 (B). a: CoB_4@Al_2O_3/air/light; b: *trans*-CoB_2A_2 @Al_2O_3/air/light; c: *cis*-CoB_2A_2 @Al_2O_3/air/light; d: CoB_3A@Al_2O_3/air/light.

in water. The carrier, the amberlite CG-400 anion-exchanged resin used often in our experiments, did not absorb these cobalt thioporphyrazines perhaps for obstruction from long chain butyl sulfide groups, therefore neutral Al_2O_3 particles were chosen as their carriers. The diffuse reflectance spectra (DRS) of the Al_2O_3 loading cobalt thioporphyrazines were shown in Fig. S13 in supplementary materials. The carrier Al_2O_3 loading cobalt thioporphyrazines showed the characteristic Q-band absorption of cobalt thioporphyrazines at near 670 nm and B-band absorption at near 355 nm respectively. It indicated that the cobalt thioporphyrazines were loaded on Al_2O_3 successfully.

3.2. Photocatalytic behavior of cobalt thioporphyrazine loaded on Al_2O_3 as biomimetic catalyst

Photocatalytic degradation of RhB in the presence of cobalt thioporphyrazines loaded on Al_2O_3 were performed at pH 4, pH 6.8 and pH 9.12 respectively.

Comparative experiments on the photocatalytic degradation of RhB in acid water of pH 4 are shown in Fig. 4. No significant change in the degradation of RhB was observed in the following reaction conditions: (1) suspension with N_2 (curve *e*); (2) in the dark (curve *f*); (3) without catalyst (curve *g*). The limited degradation of RhB with aerating N_2 or in dark maybe from the oxidation of active intermediate of the catalyst in the system [21], while the self-photosensitized oxygenation may lead to RhB degradation in the absence of catalyst. In stark contrast, more than 31% of RhB were degraded in the presence of the symmetrical catalyst CoB_4, O_2 and light irradiation (curve *a*). Therefore, it can be concluded that the degradation of RhB is a process of photocatalytic oxygenation.

Interestingly, the symmetry of cobalt thioporphyrazines also exhibited markedly different photocatalytic activity for degradation of RhB. For example, symmetrical CoB_4 showed medium photocatalytic activity with a degradation ratio of 31% after irradiation for 8 h (curve *a*), while degradation ratio of 79% was achieved for lower-symmetrical CoB_3A (curve *d* of Fig. 4). According to the degradation ratio of RhB, it can be concluded the following order of the photocatalytic activity, CoB_3A > *cis*-CoB_2A_2 > *trans*-CoB_2A_2 > CoB_4. It demonstrates that the symmetry of cobalt thioporphyrazine has a significant impact on the photocatalytic activity, namely, the lower the molecular symmetry is, the better the photocatalytic activity is.

Comparative experiments on the photocatalytic degradation of RhB using these catalysts of different symmetry were continued in neutral (pH 6.8) and basic (pH 9.12) water. These results are shown in Fig. 5. Comprehensive analysis of Fig. 5 and Fig. 4, difference of the catalytic efficiency of four cobalt thioporporazines is the largest in acid water and the least in basic water for 8 h from catalyst *a* to *d*. It implied that these catalysts are sensitive to acid and insensitive to base, perhaps hydrogen ion in acid solution beneficial to increase the catalytic activity. Anyway, they still basically maintained the order of photocatalytic activity in acid water, that is CoB_3A > *cis*-CoB_2A_2 > *trans*-CoB_2A_2 > CoB_4, though their degradation rates differed, especially the curve *c* and *d* in Fig. 5 are very close, sometimes even overlap and stagger. Moreover, similar conclusion that the photocatalytic activity of *cis*-CoB_2A_2 is higher than the activity of *trans*-CoB_2A_2 is recently reported [22].

Table 1 lists the energies of the highest occupied molecular orbitals (HOMO) and lowest unoccupied molecular orbitals (LUMO) as well as their energy gaps ($\Delta E_{H\text{-}L}$) of cobalt thioporphyrazines from DFT calculation. It is found that the $\Delta E_{H\text{-}L}$ are closely related with the catalytic activity of the cobalt thioporphyrazines, i.e.,

Table 1
Comparison of the HOMO/LUMO energies and their energy gaps with the first. Oxidation/reduction potentials and their differences of cobalt thioporphyrazines.

Compounds	E_{HOMO}(eV)[a]	E_{LUMO}(eV)[a]	$\Delta E_{H\text{-}L}$(eV)	E_{O1} (V)	E_{R1}(V)	$\Delta E_{O\text{-}R}$(V)
CoB_4	−5.758	−3.454	2.304	0.400	−0.350	0.750
trans-CoB_2A_2	−5.528	−3.296	2.232	–	–	–
cis-CoB_2A_2	−5.546	−3.327	2.219	0.430	−0.305	0.735
CoB_3A	−5.416	−3.295	2.121	0.456	−0.275	0.731

[a] The eigenvalues are averaged with the α- and β-spins.

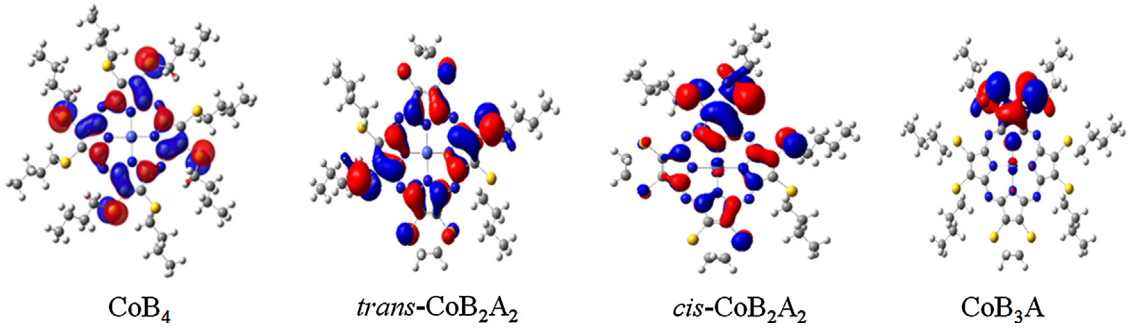

Fig. 6. The HOMOs of CoB_4, *trans*-CoB_2A_2, *cis*-CoB_2A_2 and CoB_3A calculated by the hybrid B3LYP functional level of theory.

the smaller $\Delta E_{H\text{-}L}$ indicates the higher activity of cobalt thioporphyrazine in good agreement with the order of photocatalytic activity.

In order to understand the active site of the catalyst, the HOMOs of the cobalt thioporphyrazines catalysts were analyzed in Fig. 6. It is found that all the HOMOs are significantly contributed by the lone-pairs of S atoms in the thioalkyl groups of periphery, especially for HOMO of CoB_3A that was mainly contributed from the S atoms on a pair of butylthio group of pyrrole ring opposite to dithiin ring. The electron-donating thioalkyl groups can benefit the electonic transition from HOMO to LUMO under light exitation by lowering the HOMO-LUMO gap, which facilitates the photo-generation of eletron-hole pairs and improves the photocatalytic activity.

Theoretical results also accord with those of the characterizations of UV–vis and Cyclic Voltammetric spectra. As mentioned above, asymmetric substituents of the cobalt thioporphyrazine facilated its Q-band blue-shift, especially B-band red-shift which induced by S atom in substituent groups. Electrochemical characterization of the cobalt thioporphyrazines in CH_2Cl_2 is shown in Fig. S14 in supplementary materials. Three catalysts exhibit characteristic redox behaviors at the potential range from −1.0 V to 1.0 V. The voltammetric behavior of *trans*-CoB_2A_2 was unavailable due to its low solubility in CH_2Cl_2. The electrochemical datas of different cobalt thioporphyrazines are also summarized in Table 1. Similar trends can be seen even without the data of *trans*-CoB_2A_2. According to Koopmann's theorem, the energy levels of HOMO and LUMO approximately refer to the negative value of the first oxidation potential (E_{O1}) and the first reduction potential (E_{R1}) of the molecular catalyst, respectively. Thus, the potential difference $\Delta E_{O\text{-}R}$ decreases in the order: CoB_4 > *cis*-CoB_2A_2 > CoB_3A (see Table 1), which is related to the HOMO-LUMO energy gap ($\Delta E_{H\text{-}L}$) and follows the same order as catalytic activity.

We prefered the efficiency of designed cobalt thioporphyrazine to the carrier Al_2O_3. Therefore the repeatability experiments of cobalt thioporphyrazines were not done, but their stabilities on carrier were compared. Their stabilities can be observed from the diffuse reflectance spectra (DRS) of cobalt thioporphyrazines loaded on Al_2O_3 before and after light reaction for 12 h in the absence of substrate RhB in different pH aqueous solution, shown as Fig. S15 in supplementary materials. The catalysts CoB_4@Al_2O_3 and CoB_3A@Al_2O_3 were hardly changed before and after the reactions, and the catalysts *cis*-CoB_2A_2@Al_2O_3 and *trans*-CoB_2A_2@Al_2O_3 had slightly change, whose change of peak shape may be from the catalyst to fall off because the combination between the catalyst and carrier Al_2O_3 only is physical absorption. It demonstrated that the cobalt thioporphyrazines loaded on Al_2O_3 as biomimetic catalysts are basically stable in reaction process.

The light responsivity of the metallothioporphyrazines was once performed in detail in our previous research [8]. It has been demonstrated that differed from metallophthalocyanines, metallothioporphyrazines showed light catalytic activity mainly from

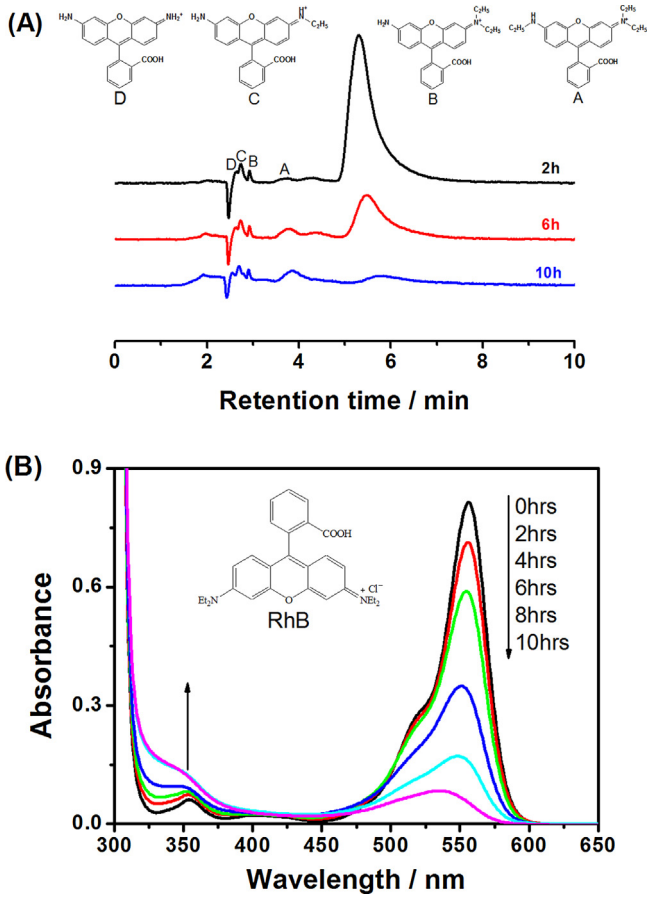

Fig. 7. The HPLC (A) and UV–vis absorption spectra (B) changes of photocatalytic degradation of RhB (1.0×10^{-5} M) with different interval for 10 h irradiation in an aerated suspension of pH 4 and in the presence of CoB_3A loaded on Al_2O_3 with loading amount of 4.0‰.

weak UV light among Xe lamp simulating sunlight. The similar result was also obtained using the CoB_3A@Al_2O_3 as an exsample (see Fig. S16 in supplementary materials), degradation of RhB was donated less from visible light and maily form the light of lower than 400 nm.

3.3. 3 A possible photocatalytic mechanism of cobalt thioporphyrazine loaded on Al_2O_3

HPLC was employed further to study the degraded products of photooxidation, shown in Fig. 7(A). The HPLC of the degraded products from RhB was similar with our previous results [7]. At 2 h, four main components *N*,*N*-diehyl-*N*- ethyl-rhodamine (product A, retention time: 3.84 min), *N*,*N*-diethyl-rhodamine (product B,

retention time: 2.9 min), *N*-ethyl-rhodamine (product C, retention time: 2.67 min), rhodamine (product D, retention time: 2.5 min) were detected by HPLC using a reversed-phase C18 column at 500 nm. Seeing from the HPLC, it was found that RhB was rapidly degraded and hardly any RhB was remained after 10 h. The amount of product A was increased from 2 h to 6 h, and then it decreased gradually. However, the amount of other degradation products, such as B, C and D which were formed from the further de-ethylation of product A, were almost stable during the degradation process. These results indicated that product A was the main intermediate during the degradation of RhB. The possible mechanism of degradation was that N,N-diehyl-N-ethyl-rhodamine (product A) was the main intermediate, which was directly cleaved by reactive oxidizing species.

For an example of the CoB_3A, the degradation process was discussed. Fig. 7(B) shows the UV–vis absorption spectra of the RhB in the presence of CoB_3A loaded on Al_2O_3 at various intervals during 10 h irradiation. It is observed that the characteristic λ_{max} of RhB at 556 nm decreased continuously with some hypsochromic shifts, which is attributed to the de-ethylation assigned to the formation of some degraded species of the molecule's framework [7]. Meanwhile, the absorbance for degraded products in the UV region increased during the irradiation process. The degradation rate of RhB could reach about 93% after irradiation for 10 h. These results clearly exhibit the chromophores of RhB were effectively cleaved. It demonstrates that effective degradation of RhB was photocatalyzed by the CoB_3A loaded on Al_2O_3 under light irradiation in an aerated suspension.

To illustrate the effect of mudulation of peripheral substituents on the photocatalytic activity of cobalt thioporphyrazines, the active species were examined in the presence of cobalt thioporphyrazines respectively. The coumarin readily reacts with hydroxyl radical ($HO^{\bullet}$) to produce highly fluorescent product, which has been extensively used to detect HO· in aqueous solution [23]. But the HO· was not detected by the fluorescent technology of coumarin in these degraded solutions in the presence of cobalt thioporphyrazines respectively (see Fig. S17 in supplementary materials). Meanwhile, no obvious signals of $HO^{\bullet}$ were detected by ESR technology of free radical trapping in the presence of cobalt thioporphyrazines respectively. However, strong signals of singlet oxygen ($^1O_2$) were detected by ESR technology, shown in Fig. 8(A). It is implied that the $^1O_2$ is main reactive oxygen species (ROS) in the presence of the catalyst. And the $^1O_2$ singals showed the marked difference for different substituent groups of cobalt thioporphyrazines. From Fig. 8(A), it could be seen that the signal intensity of $^1O_2$ follows the order for cobalt thioporphyrazines under the same conditions: CoB_3A > *cis*-CoB_2A_2 > *trans*-CoB_2A_2 > CoB_4, which is consistent with the order of photocatalytic activity. Meanwhile, the superoxide anion radical ($O_2^{-\bullet}$) was also measured by ESR technology, shown in Fig. 8(B). The characteristic sixfold peak could be observed though the $O_2^{-\bullet}$ singals were weaker in the presence of the catalyst, it could seen that the signal intensity of $O_2^{-\bullet}$ for asymmetrical cobalt thioporphyrazine is still stronger than that for symmetrical one. It same means that the ability of activating dioxygen of the cobalt thioporphyrazine is closely related to the symmetry of molecular structure, and the molecule of catalyst stimulated by light not only occurred energy transfer but also produced electron transfer to oxygen.

Therefore, a possible mechanism that cobalt thioporphyrazine activates O_2 for degradation of dye RhB was prosposed. There were two paths for cobalt thioporphyrazine activating O_2, one is the catalyst as sensitizer to produce energy transfer to O_2 forming $^1O_2$, the other is the catalyst to occur electron transfer to O_2 producing $O_2^{-\bullet}$ under light irradiation, in which an electron was excited from HOMO jumping to LUMO when the catalyst was irradiated by light, then the electron transmitted to O_2 from the LUMO to form $O_2^{-\bullet}$,

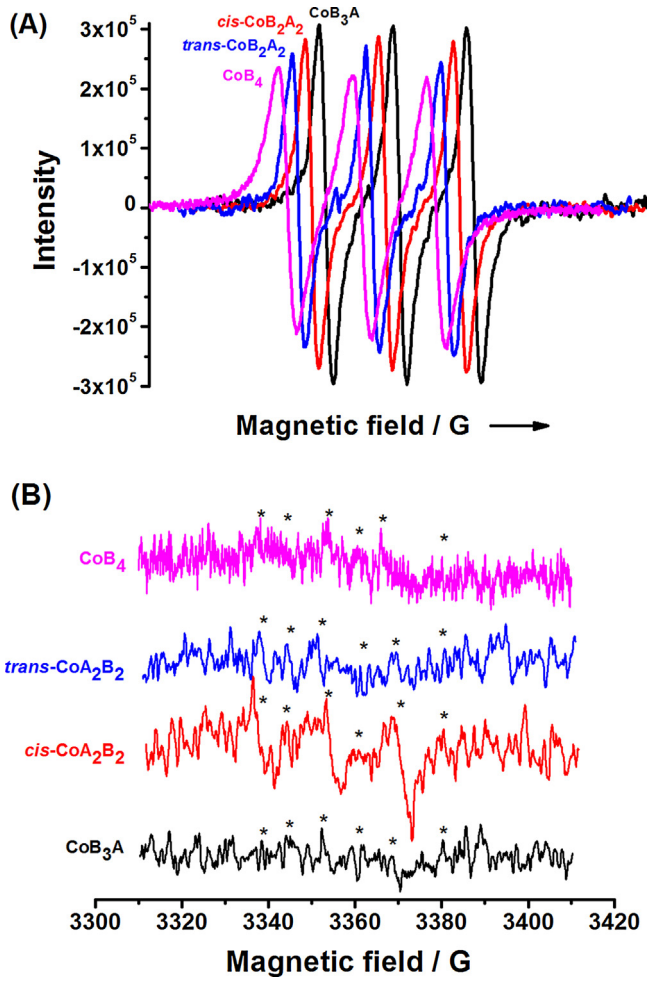

Fig. 8. ESR spectra of DMPO adduct with $^1O_2$ (A) and TMP adduct with $O^{2-\bullet}$ (B) generated in the potocatalytic process in the presence of Al_2O_3 loaded cobalt thioporphyrazines. Reaction conditions: 5 mg cobalt thioporphyrazine loaded on Al_2O_3 was added into 4 mL methanol, then 60 μL DMPO or 20 μL TMP was added in an aerated suspension with oxygen. (Note: in order to compare the relative strength of the $^1O_2$ signals, the parallel translation about 4 G of the abscissa).

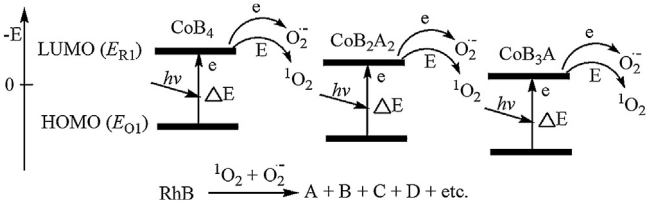

Fig. 9. The cobalt thioporphyrazines with different substituent groups in the macrocyclic periphery had obviously effect on the energy gaps ΔE of frontier orbitals, leading to change the catalytic activity.

then oxidating dye RhB into small fragments such as A, B, C, D and etc. Obviously, the former is dominant, shown as Fig. 9.

4. Conclusions

In this study, a series of symmetrical and asymmetrical cobalt thioporphyrazines through modulation of peripheral substituents have been synthesized by the Linstead's template method, which show capability of activating dioxygen under irradiation of the Xe lamp simulating sunlight. Loaded on Al_2O_3 as photocatalyst, the lower- symmetrical cobalt thioporphyrazine displays higher capability to activate dioxygen than that of the symmetrical struc-

ture in the degradation of dye RhB under different pH solution conditions. It is demonstrated that the mudulation of peripheral substituents of thioporphyrazine has a moderate impact on the energy gaps ($\Delta E_{H\text{-}L}$) of their frontier orbitals and the contribution of S atom in substitiuents to HOMO of the obtained photocatalyst. Lowering the molecular symmetry of the cobalt thioporphyrazines moderately decreased the HOMO-LUMO energy gap and increased the contribution of S atom in substitiuents to HOMO so as to enhance the photocatalytic activity in degradation of organic dye RhB: CoB_3A > *cis*-CoB_2A_2 > *trans*-CoB_2A_2 > CoB_4, among which the asymmetric $CoAB_3$ can effectively catalyze to degrade About 93% of the RhB at pH 4 for 10 h.

With the aid of ESR technology of free radical trapping and DFT calculation, it demonstrates that the $^1O_2$ and $O_2^{-\bullet}$ are main ROS in the presence of the catalyst. The distribution of $^1O_2$ and O_2^- is depended on the energy difference ($\Delta E_{H\text{-}L}$) of frontier orbitals of the catalyst, which is further closely related to the photocatalytic activity under simulating sunlight irradiation. The cobalt thioporphyrazines showed light catalytic activity mainly from weak UV light among Xe lamp simulating sunlight. In the current system, the activation of dioxygen is divided into two paths: one is the catalyst as sensitizer to produce energy transfer to O_2 forming $^1O_2$; the other is the catalyst to occur electron transfer to O_2 producing $O_2^{-\bullet}$. The former is dominant path according to the intensity of ESR signals of ROS. Through analysis of degraded products by HPLC, a possible degradation mechanism of dye RhB is also proposed.

The work not only obtains some effective biomimetic catalysts, but also provides a reference in designing highly effective photocatalyst based on metalloporphyrin-like.

Acknowledgements

This work was finally supported by the National Natural Science Foundation of China (Nos. 20377053 and 205770703), Natural Science Foundation of Hubei Province, PR China (2014CFB919) and "the Fundamental Research Funds for the Central Universities", South-Central University for Nationalities (CZY14003).

Appendix A. Supplementary data

Supplementary data associated with this article can be found, in the online version, at http://dx.doi.org/10.1016/j.apcatb.2016.03.059.

References

[1] Y. Rio, M.S. RodÍguez-Morgade, T. Torres, Org. Biomol. Chem. 6 (2008) 1877–1894.
[2] M.J. Fuchter, C. Zhong, H. Zong, B.M. Hoffman, A.G.M. Barrett, Aust. J. Chem. 61 (2008) 235–255.
[3] R. Su, J. Sun, Y. Sun, K. Deng, D. Cha, D. Wang, Chemosphere 77 (2009) 1146–1151.
[4] Z. Zhang, Q. Peng, J. Sun, L. Fang, K. Deng, Ind. Eng. Chem. Res. 52 (2013) 13342–13349.
[5] C. Yang, J. Sun, K. Deng, D. Wang, Catal. Commun. 9 (2008) 321–326.
[6] L. Chen, Z. Zhang, Y. Wang, Y. Guan, K. Deng, K. Lv, J. Sun, Z. Li, M. Li, J. Mol. Catal. A: Chem. 372 (2013) 114–120.
[7] Z. Zhang, M. Zhang, J. Deng, K. Deng, B. Zhang, K. Lv, J. Sun, L. Chen, Appl. Catal. B: Environ. 132 (2013) 90–97.
[8] Z. Zhang, X. Wen, K. Deng, B. Zhang, K. Lv, J. Sun, Catal. Sci. Technol. 3 (2013) 1415–1422.
[9] V. Král, J. Králová, R. kaplánek, T. Bříza, P. Martáser, Physiol. Res. 55 (2006) S3–S26.
[10] N. Tripathy, R. Ahmad, J. Eun Song, H. Ah Ko, Y.-B. Hahn, G. Khang, Mater. Lett. 136 (2014) 171–174.
[11] S. Wang, D. Li, C. Sun, S. Yang, Y. Guan, H. He, Appl. Catal. B: Environ. 144 (2014) 885–892.
[12] W. Yuan, X. Liu, L. Li, Appl. Surf. Sci. 319 (2014) 350–357.
[13] C. Chen, W. Ma, J. Zhao, Chem. Soc. Rev. 39 (2010) 4206–4219.
[14] K. Rajeshwar, M. Osugi, W. Chanmanee, C. Chenthamarakshan, M.V.B. Zanoni, P. Kajitvichyanukul, R. Krishnan-Ayer, J. Photochem. Photobiol. C 9 (2008) 171–192.
[15] S. Mandal, S.K. Nayak, S. Mallampalli, A. Patra, ACS Appl. Mater. Interfaces 6 (2013) 130–136.
[16] Y. Zhong, J. Wang, R. Zhang, W. Wei, H. Wang, X. Lü, F. Bai, H. Wu, R. Haddad, H. Fan, Nano lett. 14 (2014) 7175–7179.
[17] Y. Zhong, Z. Wang, R. Zhang, F. Bai, H. Wu, R. Haddad, H. Fan, ACS Nano 8 (2014) 827–833.
[18] T.F. Baumann, M.S. Nasir, J.W. Sibert, A.J.P. White, M.M. Olmstead, D.J. Williams, A.G.M. Barrett, B.M. Hoffman, J. Am. Chem. Soc. 118 (1996) 10479–10486.
[19] J. Mack, M.J. Stillman, The Porphyrin Handbook, Vol.16, 2003, pp. 43–116 (Chapter103).
[20] L. Zhang, D. Qi, L. Zhao, Y. Bian, W. Li, J. Mol. Graphics Modell. 35 (2012) 57–65.
[21] The cobalt thioporphyrazine can be slightly oxygenated to produce the active intermediate of thioporphyrazine with a sulfoxide group in air, which can transfer the oxygen in sulfoxide group to oxidate organic molecules in dark or N_2 atomsphere. We have observed the phenomenon, which is being studied further for publish.
[22] L. Luo, R.B. Ambre, S.B. Mane, E.W. Diau, C. Hung, Phys. Chem. Chem. Phys. 17 (2015) 20134–20143.
[23] I. Rosenthal, E. Ben-Hur, Int. J. Radiat Biol. 67 (1995) 85–91.